# On the Connection between Dense Water Formation, Overturning, and Poleward Heat Transport in a Convective Basin*

FIAMMETTA STRANEO

*Department of Physical Oceanography, Woods Hole Oceanographic Institution, Woods Hole, Massachusetts*

(Manuscript received 21 March 2005, in final form 5 January 2006)

ABSTRACT

An isopycnal, two-layer, idealized model for a convective basin is proposed, consisting of a convecting, interior region and a surrounding boundary current (buoyancy and wind-driven). Parameterized eddy fluxes govern the exchange between the two. To balance the interior buoyancy loss, the boundary current becomes denser as it flows around the basin. Geostrophy imposes that this densification be accompanied by sinking in the boundary current and hence by an overturning circulation. The poleward heat transport, associated with convection in the basin, can thus be viewed as a result of both an overturning and a horizontal circulation. When adapted to the Labrador Sea, the model is able to reproduce the bulk features of the mean state, the seasonal cycle, and even the shutdown of convection from 1969 to 1972. According to the model, only 40% of the poleward heat (buoyancy) transport of the Labrador Sea is associated with the overturning circulation. An exact solution is presented for the linearized equations when changes in the boundary current are small. Numerical solutions are calculated for variations in the amount of convection and for changes in the remotely forced circulation around the basin. These results highlight how the overturning circulation is not simply related to the amount of dense water formed. A speeding up of the circulation around the basin due to wind forcing, for example, will decrease the intensity of the overturning circulation while the dense water formation remains unvaried. In general, it is shown that the fraction of poleward buoyancy (or heat) transport carried by the overturning circulation is not an intrinsic property of the basin but can vary as a result of a number of factors.

## 1. Introduction

Open-ocean convective regions, such as the Greenland Sea, the Labrador Sea, or the northwest Mediterranean, are thought to play a role in the global or local thermohaline circulations. Perhaps more significant, the large loss of heat to the atmosphere, occurring in these regions, contributes to the poleward heat transport by the ocean, and the water mass transformation (densification) generates meridional density gradients that are associated with the meridional overturning circulation (MOC). In terms of variability, general circulation models show a strong correlation between variations in water mass transformation in such regions and both the poleward heat transport and MOC. For example, a strengthening of convection in the Labrador Sea will precede an intensification of the MOC and poleward heat transport (Eden and Willebrand 2001; Bentsen et al. 2004). In practice, however, the causality and details of this connection are still poorly understood, and there is no dynamical theory relating the amount of dense water formed with the overturning circulation or the poleward heat flux. We cannot explain, for example, why a decrease of 8–9 Sv (Sv $\equiv 10^6$ $m^3\ s^{-1}$) in Labrador seawater (LSW) formation, in one model, is associated with a smaller decrease (5–6 Sv) in the MOC (Mauritzen and Hakkinen 1999).

A related confusing aspect of the problem involves the distinction between dense water formation (a diapycnal mass flux) and sinking (here intended as a vertical mass flux). Historically, convective regions were identified as regions where water is made dense by buoyancy loss to the atmosphere, sinks (to the bottom or to its neutral density level), and spreads away from

* Woods Hole Oceanographic Institution Contribution Number 11304.

*Corresponding author address:* Dr. Fiammetta Straneo, Woods Hole Oceanographic Institution, Mail Stop 21, Woods Hole, MA 02543.
E-mail: fstraneo@whoi.edu

the formation region, thus requiring a surface return flow. In reality, however, widespread sinking in the open ocean is strongly inhibited on a rotating planet both during convection (Send and Marshall 1995; Spall and Pickart 2001) and during the postconvective adjustment phase (Spall 2004). Sinking of the dense water can, on the other hand, occur at the topographic boundaries of convective basins but it is unclear what parameters control the fraction of dense water formed that will sink (Spall 2004; Pickart and Spall 2006, manuscript submitted to *J Phys. Oceanogr.,* hereinafter PS06).

On a more positive note, a large amount of data have been collected in at least one open-ocean convective basin, the Labrador Sea, over the last decade (e.g., Lab Sea Group 1998). Analysis of these data, in conjunction with a series of orchestrated numerical and laboratory experiments, has greatly improved our understanding of how an open-ocean convection site works and how it is connected to the larger scale circulation. The general picture that emerges from these studies is the following. Deep/intermediate convection occurs primarily in the interior of the basin (Pickart et al. 2002; Rhein et al. 2002), in a region with little or no mean flow (Lavender et al. 2000). At the edges of the basin, a cyclonic boundary current system provides the conduit for the advection of buoyant water into the basin (to balance the net annual buoyancy loss to the atmosphere) and for the export of dense water out of the basin (Lazier and Wright 1993; Cuny et al. 2002). Instability of the boundary current is thought to be the dominant process regulating the exchange of properties between the interior and the boundary current (Eden and Böning 2002; Lilly et al. 2003; Spall 2004; Katsman et al. 2004). The boundary current and its instability thus play a fundamental role within this new paradigm, to be contrasted with the earlier paradigm of isolated convection forced by a localized buoyancy forcing (Jones and Marshall 1993, 1997; Maxworthy and Narimousa 1994).

This study is aimed at using this new paradigm to explicitly relate dense water formation in a convective basin with thermohaline-circulation-related quantities, which include the meridional overturning circulation and the poleward heat flux. To do this, I introduce a simplified model for an open-ocean, semienclosed convective basin. The model is designed to fit the Labrador Sea case, but its formulation is generic and applicable to other convecting basins sharing similar large-scale features, such as the northwest Mediterranean or the Greenland Sea (Marshall and Schott 1999). It includes an interior region, where convection occurs, and a surrounding boundary current that is both buoyancy driven (by convection in the basin) and remotely driven (e.g., by wind). The model assumes that the boundary current is the only means by which buoyant water is advected into the basin, and dense water is removed from the basin. As a result, the boundary current must "give up" buoyant water and collect dense water as it circles around the basin, resulting in an alteration of its baroclinic structure. A number of linear and nonlinear solutions for the boundary's current transformation are presented in this study. Support for the model's formulation is given by its ability to reproduce many of the observed bulk features of the Labrador Sea. One important dynamical consequence of the densification of the boundary current, as it circles the basin, is that some fluid has to sink for the flow to remain in geostrophic balance. This sinking, or downwelling, is what drives a net overturning circulation within the basin and is hence relevant to studies of thermohaline circulation variability, As explicitly shown here, the fraction of poleward heat transport carried by this overturning circulation is not fixed by the basin's configuration but varies with a number of parameters, including the mean circulation. This suggests a coupling between the buoyancy- and wind-driven circulation in shaping the overturning associated with convection.

The new paradigm, and observations that support it, are discussed in section 2. The model is presented in section 3, and its ability to reproduce the observed mean state, seasonal cycle, and shutdown of convection observed in the Labrador Sea is discussed in section 4. The basic model dynamics are discussed in section 5 by presenting a linearized solution, and numerical solutions for a range of parameters. A summary of the findings of this study is presented in section 6, and a discussion of their implications is presented in section 7.

## 2. Essential elements of a convective basin

### *a. Building on the Labrador Sea case*

The simplified representation of a convective basin utilized in this study was suggested by piecing together observations from, and modeling studies adapted to, the Labrador Sea. These studies are now briefly reviewed here to illustrate that the Labrador Sea does indeed fit the basic paradigm referred to above. At the same time, there is nothing particular about the Labrador Sea that would imply that this representation is pertinent to it alone. Instead the well-known similarities between the various open-ocean convection regions (Marshall and Schott 1999) suggest that it can be applied to these regions too.

The Labrador Sea is a well-known region of intermediate/deep convection resulting in the formation of an intermediate dense water, LSW (Lazier 1980) found

throughout much of the subpolar North Atlantic Ocean and beyond (Talley and McCartney 1982). The water mass transformation associated with LSW is thought to play a significant role in the poleward heat transport and overturning circulation of the North Atlantic (Talley 2003).

### b. *Two regimes: The interior and the boundary current*

The Labrador Sea can be decomposed in two distinct regions, the interior and the boundary current, characterized by different circulation and properties distribution. Lagrangian measurements show that the mean circulation is confined to its lateral, topographic boundaries with essentially no mean inflow into the interior (Lavender et al. 2000). Hydrographic surveys show the interior region to be mostly horizontally homogeneous[1] with strong lateral density gradients confined again to the topographic boundaries (Pickart et al. 2002; Lazier et al. 2002). These gradients separate cold interior waters from warm waters (modified North Atlantic Current water known as Irminger Water) advected by the boundary current into the region (Lazier et al. 2002; Cuny et al. 2002). The boundary current is also instrumental in advecting the remnants of the Irminger Water out of the basin along with the convectively produced LSW water (Lazier and Wright 1993; Lazier et al. 2002).

The boundary current circulation in the Labrador Sea has a strong barotropic character, which can be attributed to the wind-driven return flow of the subpolar gyre (Lazier and Wright 1993). The net transport is on the order of 30 Sv (see Pickart et al. 2002, and references therein), of which about 14 Sv occur in the deepest waters from the overflows, leaving approximately 12 and 4 Sv to be transported within the upper (light) and LSW layers (PS06).

### c. *Convection and restratification of the interior*

The bulk of LSW is formed during winter in the interior (Clarke and Gascard 1983; Pickart et al. 2002; Rhein et al. 2002) by a large surface buoyancy loss. It is important to realize that the formation (or transformation) is primarily associated with a diapycnal mass flux (i.e., densification of waters) but not with a vertical mass flux (downwelling or sinking). During active convection, sinking of dense fluid within the plumes' core is balanced by upwelling around them. This is supported both by observations during active convection (Send and Marshall 1995) as well as by nonhydrostatic numerical simulations that explicitly resolve plumes (Spall 2003, 2004). Also, it is consistent with theoretical considerations, based on planetary geostrophy, which show how a widespread downwelling in the ocean's interior would have to be balanced by an unrealistically large horizontal circulation (Send and Marshall 1995; Spall and Pickart 2001).

Following the large wintertime diapycnal mass flux, the Labrador Sea's interior restratifies, that is, becomes more buoyant, primarily[2] through lateral exchange with the boundary current (Lazier et al. 2002; Straneo 2006). This exchange is thought to be dominated by mesoscale eddies, as supported by observations (Lilly et al. 1999; Prater 2002; Lilly et al. 2003), and by the numerical simulations (from idealized to more realistic) of Khatiwala and Visbeck (2000), Spall (2004), Katsman et al. (2004), and Eden and Böning (2002). In principle, this eddy exchange could be associated with a net vertical mass flux (as suggested by Khatiwala and Visbeck 2000). Again, however, both scalings and nonhydrostatic simulations show that this is not the case and that eddies are very inefficient in driving a vertical mass flux in the open ocean (Spall 2003, 2004).

### d. *The boundary current transformation*

The boundary current is the primary conduit for the export of LSW out of the basin (Straneo et al. 2003) and, as such, it must lose buoyant water and gain LSW[3] as it travels around the basin (Cuny et al. 2002). This exchange, as argued above, is primarily governed by eddies. Eddy-resolving numerical simulations show that these eddies result both in a net densification of the current and in driving a downward mass flux through their interaction with topography (Spall 2003, 2004). The latter occurs in a thin boundary layer close to topography where frictional constraints allow vorticity to be dissipated (Spall and Pickart 2001; Spall 2004). The bulk characteristics of the transformation process, however, are found not to be overly sensitive to the details of the small-scale diffusive and viscous parameterizations (Spall 2004).

[1] The large degree of homogeneity in the interior can in part be attributed to the rapid and efficient mixing observed at moorings acting to remove lateral structures within a few months after convection (Lilly et al. 1999), and justified on the basis of the energetic eddy structures left over after convection (Legg and McWilliams 2001).

[2] The restratification due to solar heating is trapped to a thin surface layer (Straneo 2006).

[3] Densification of the boundary current can also result from surface buoyancy losses occurring directly over it (especially off of the Labrador coast: Straneo et al. 2002; Cuny et al. 2002; Brandt et al. 2004) but the extent to which this occurs is still unclear. Hence, in this study, it is assumed to be primarily due to lateral exchange with the interior.

*e. A two-layer system*

While the vertical structure of the Labrador Sea (both in the interior and in the boundary current) comprises four distinct layers (a surface cold, fresh layer; a warm, salty intermediate layer; LSW layer; and a layer of denser waters from the overflows), I will argue that the convective cycle can be effectively represented by two layers alone (the warm, salty intermediate layer and the LSW layer).

The dense North Atlantic Deep Water (NADW), from the Nordic seas overflows, circulates around the basin at depth, in the deep western boundary current (Lazier and Wright 1993), and fills the bottom of the sea's interior. These waters are not reached by convection except during extreme events [e.g., in 1993, after the intense winters of the early 1990s (Lazier et al. 2002)] and, hence, do not typically participate in LSW formation and export.

The layer of cold, fresh, surface waters circulating around the basin, in the West Greenland and Labrador Currents, does, on the other hand, play a role in the basin's convective cycle. However, it is argued here that its role is a mostly thermodynamic one, as opposed to a truly dynamical one; hence it can be accounted for by modifying the surface forcing conditions. In the boundary current, these buoyant surface waters tend to prevent convection—a feature that is taken into account by assuming that no water mass transformation occurs there (or equivalently that the surface buoyancy flux over the boundary current is zero). In the interior, these surface waters contribute (together with net precipitation) to the seasonal restratification (Lazier 1980) and to the properties of LSW via their wintertime destruction. In terms of dynamics, however, this layer is, at most, a few tens of meters thick and its contribution to horizontal density gradient is negligible relative to that of the Irminger Water/LSW layer gradients. Hence this layer acts mostly as a thermodynamic filter [and anomalies in this layer's properties can contribute to the shutdown of convection, e.g., during the Great Salinity Anomaly (Lazier 1980)] but not directly as a dynamically active layer.

Indeed, the bulk of available potential energy stored in the basin is due to the LSW being thicker in the interior than in the boundary current (at the expense of the Irminger Water layer). This is supported by the recent analysis of Straneo (2006) who shows that the interannual variability in the restratification can be related to the interior/boundary current Irminger Water/LSW thickness difference. It is also consistent with the general description of the seasonal restratification via the advection, into the interior, of modified Irminger Water of Khatiwala et al. (2002) and Lilly et al. (1999).

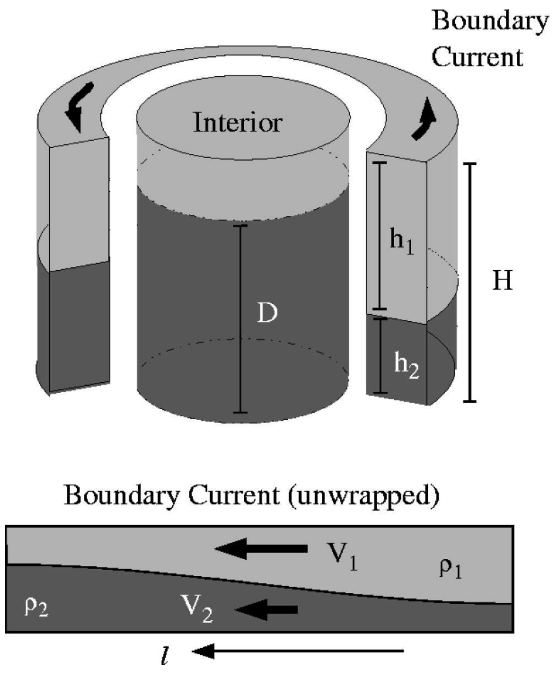


FIG. 1. Schematic of the two-layer model.

*f. Summary*

Following the discussion above, the model that is proposed here as representative of the dynamics of a convective basin is the following. The system is described in terms of two layers, a light water mass and a dense water mass (respectively representing Irminger and Labrador seawater) and of two distinct regions: an interior region and a boundary current that surrounds it (Fig. 1). Properties are assumed to be horizontally homogeneous within the two regions.

Convection is limited to the interior region and is associated with a conversion of light water into dense water with no associated vertical mass flux. Thus convection increases the reservoir of dense water in the interior, creating or, more exactly, maintaining a thickness gradient between the interior and the boundary current. Flow into and out of the basin occurs in the boundary current and is both wind and buoyancy driven. For simplicity, the wind-driven flow is assumed to be barotropic. The mostly adiabatic exchange between these two regions is regulated by instabilities attempting to flatten the interior/boundary current gradient. These result in a net flux of buoyancy into the basin's interior that balances the net annual buoyancy loss.

## 3. Model formulation

### a. Model parameters and variables

Let $\rho_1$ and $\rho_2$ be the respective densities of the light layer (Irminger Water) and of the dense (LSW) layer, and let $\Delta\rho = \rho_2 - \rho_1$. The basin's geometry is assumed to be cylindrical, with a total depth $H$, interior area $A = \pi R^2$, and a boundary current of thickness $L$ and total perimeter $P$. The variables of the system are the interior's dense water thickness $D(t)$ and the boundary current's layer thicknesses [$h_1(l, t)$ and $h_2(l, t)$] and velocities [$V_1(l, t)$ and $V_2(l, t)$], Fig. 1, where $l$ is the along-boundary coordinate ranging from 0 to $P$. Because it is assumed that sea surface height variations are negligible around the basin, it follows that the layer thicknesses are simply related by $h_1(l, t) = H - h_2(l, t)$. The sea surface height difference between the interior and the boundary is assumed negligible compared to variations in the layer thicknesses. The model equations are formulated separately for the interior and boundary current and a closure scheme is used to parameterize the exchange between the two.

### b. Interior

Following the considerations above, it is assumed that there is no mean flow into the interior. Properties within the interior can thus be described by a single conservation equation for buoyancy (or heat):

$$\frac{\partial}{\partial t}\int_V \overline{\rho}\, dV + \int_P \int_H \overline{u'\rho'}\, dz\, dl = \frac{\rho_0}{g}\int_A Q_b\, dS, \tag{1}$$

where density is used instead of buoyancy for simplicity, $V$ is the interior volume, $\rho$ is density, $\rho_0$ is a reference density for seawater, $g$ is gravity, $Q_b$ is the surface buoyancy flux (positive implies a buoyancy loss by the ocean), and $u'\rho'$ are the eddy fluxes of density ($\overline{u'\rho'} > 0$ implies lightening, or warming, of the interior). The overbars indicate averaging over typical eddy time scales. This formulation has already been utilized in a number of modeling studies including Jones and Marshall (1997), Visbeck et al. (1996), Khatiwala et al. (2002), and Spall (2004). Given the model's two layers and the assumption that the interior is homogeneous, this becomes

$$\Delta\rho\frac{dD}{dt} + \frac{1}{A}\int_P \int_H \overline{u'\rho'}\, dz\, dl = \frac{\rho_0}{g} Q_b, \tag{2}$$

where the surface buoyancy flux $Q_b$ is assumed to be spatially uniform over the interior and $D$ is the dense layer's thickness in the interior.

### c. Boundary current

The goal of this study is to understand how the boundary current changes around the basin as a result of convection in the interior. The two-layer model described here is intended to represent the bulk features of the current. The premise behind this formulation is that these features are imposed by the large-scale dynamics and thermodynamics of the problem and not governed by the small-scale physics. Explicitly, the assumption is that, while the model does not include a detailed description of the thin boundary layer where the downwelling is thought to occur, it can still be used to diagnose the net downwelling and associated diapycnal mass flux. This formulation is supported by the aforementioned studies [and, in particular, those of Spall (2003, 2004)], which suggest that what happens in the boundary layer is determined by the large-scale dynamics and thermodynamics, and not the other way around.

#### 1) CONTINUITY

Let ($u$, $v$, $w$) be the velocity components in the across-stream, along-stream, and vertical directions, respectively, associated to the following spatial variables and respective ranges: $r \in [0, L]$, $l \in [0, P]$ and $z \in [0, -H]$. In the across-stream direction, it is assumed that there is no mean exchange with the interior ($u(0, l, z) = 0$) and that there is no flow into the lateral solid boundary [$u(L, l, z) = 0$]. The continuity equation can therefore be integrated across the boundary current width to yield

$$V_l + W_z = 0,$$

where $V$ and $W$ indicate velocities averaged in the across-stream direction. Vertical integration (between $z = 0$ and $z = -H$) of the above expression yields

$$\frac{\partial}{\partial l}(V_1 h_1 + V_2 h_2) = 0, \tag{3}$$

that is, volume conservation. In the Boussinesq approximation this is equivalent to mass conservation. (For a typical boundary current transport of 20 Sv, the difference in transport by assuming that mass instead of volume is conserved is of the order of 1 mSv and thus negligible for all purposes of this study.) The vertical velocity at any given depth can be derived from continuity:

$$W(z) = -\int_{-H}^{z} \frac{\partial V}{\partial l}\, dz,$$

where $W(H) = 0$ and the downwelling across the layer interface, $z = -h_1(l)$, is given by

$$W_i = -\int_{-H}^{-h_1} \frac{\partial V}{\partial l}\, dz = -h_2 \frac{\partial V_2}{\partial l}. \tag{4}$$

### 2) Buoyancy conservation

A statement for the conservation of buoyancy in the boundary current is constructed as follows. It is assumed that the light layer is isolated from the surface forcing, so any changes in this layer must be due to lateral exchange with the interior or to an exchange with the dense layer beneath. Similarly, for the dense layer, any change in thickness must be due either to lateral exchange or to exchange with the light layer. Instead of using separate equations for the two layers, however, only the vertically integrated buoyancy content of the current is considered here. As a result the term describing the diapycnal exchange between the two layers (i.e., $w\partial\rho/\partial z$) does not appear explicitly but is included in the divergence term. (If one had retained separate equations for the two layers, the vertical diapycnal mass flux into each layer would have appeared as a source/sink term on the right.)

The statement for the conservation of buoyancy, integrated both vertically and across the current width, becomes

$$\frac{\partial}{\partial t}\int_L \int_H \overline{\rho}\, dz\, dr + \int_L \int_H \frac{\partial}{\partial l}(\overline{v\rho})\, dz\, dr = -\int_H \overline{u'\rho'}\, dz, \tag{5}$$

where $L$ is the boundary current width and $l$ is the along-stream variable. In deriving this expression, it has been assumed that there is no mean flow between the boundary current and the interior and that the lateral eddy fluxes are the principal driver for changes in the boundary current. Using volume conservation, this becomes

$$L\Delta\rho \frac{\partial h_2}{\partial t} + L\Delta\rho \frac{\partial}{\partial l}(V_2 h_2) = -\int_H \overline{u'\rho'}\, dz, \tag{6}$$

where properties have been averaged across the current and overbars indicating temporal averages have been dropped.

### 3) Geostrophy

The flow in the boundary layer is represented in terms of the mean velocities within each layer. It is assumed that changes in thickness in the interior and in the boundary current occur over time scales that are much longer than a day so that the flow is always geostrophically adjusted. Let $V_1$ and $V_2$ be the mean flow components in the along-stream directions. For simplicity, the model is formulated in terms of the average (across the current's width) layer thicknesses. In practice, however, the layer thickness will slope across the boundary current so that the baroclinic velocity, assumed in geostrophic balance, is

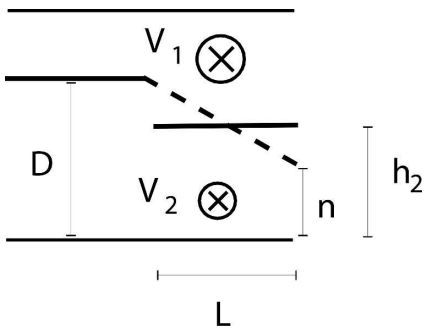


FIG. 2. Schematic illustrating the relation between the thickness slope $[(D - n)/L$, dashed line] across the boundary current and the mean thickness across the current $h_2$.

$$V_{\text{bcl}} = V_1 - V_2 = \frac{g'}{fL}(D - n),$$

where $n$ is the dense layer thickness at the edge of the boundary current (see Fig. 2) and $g' = g\Delta\rho/\rho_0$ is the reduced gravity. If described in terms of $h_2$, the mean layer thickness across the boundary current, then the baroclinic velocity becomes

$$V_{\text{bcl}} = V_1 - V_2 = \frac{2g'}{fL}(D - h_2) = v^* \frac{(D - h_2)}{H},$$

where $v^* = \dfrac{2g'H}{fL}$

is a measure of the magnitude of the baroclinic flow. The total barotropic velocity, defined as the vertically averaged velocity, is given by

$$V_{\text{btp}} = \frac{V_1 h_1 + V_2 h_2}{H},$$

and the individual layer velocities can be obtained using

$$V_1 = V_{\text{btp}} + \frac{h_2}{H} V_{\text{bcl}} \quad \text{and} \quad V_2 = V_{\text{btp}} - \frac{h_1}{H} V_{\text{bcl}}.$$

Since the interface slopes around the basin's perimeter, it follows that there also exists a mean pressure gradient in the along-flow direction and, hence, a geostrophic flow associated with it:

$$u_{\text{bc}} = u_1 - u_2 = \frac{g'}{f}\frac{\partial h_2}{\partial l}.$$

Note that this is not inconsistent with the assumption that there is no mean exchange between the boundary and the interior. Indeed, if one assumes that there is no discontinuity at the interior/boundary current "boundary," then $h_2(r = 0, l) = D$ for every $l$. In essence, the outer portion of the boundary current smoothly matches the interior conditions and the along-stream slope of the interface is flat where the two regions meet. This also means that at this boundary $u_{\rm bc}(r = 0, l) = 0$, which is consistent with the no mean exchange. Moving away from the interior and toward the solid boundary, the layer interface starts sloping in the along-stream direction and there must be a geostrophic flow in the across-stream direction. At the solid boundary this flow must go to zero, $u_{\rm bc}(r = L, l) = 0$. How it goes to zero will depend on the details of the viscous dissipation in the thin boundary layer. A detailed description of these boundary layer processes is beyond the purpose of this study; the assumption (supported by the numerical simulations described above) is that they do not affect the bulk characteristics of the solution. At the same time, it is important to realize that the present formulation is self-consistent in that it satisfies the specified boundary conditions.

### d. Eddy flux parameterization

Following Spall (2004) and references therein, it is assumed that the eddy fluxes are proportional to the isopycnal slope between the interior and the boundary current:

$$\overline{u'\rho'}(z, l, t) = c\delta\rho(z)V_{\rm bcl} = c\delta\rho(z)\upsilon^* \frac{D - h_2}{H}, \quad (7)$$

where $c$ is an efficiency coefficient tied to the topographic slope (Spall and Chapman 1998; Spall 2004) and $\delta\rho(z)$ is the density difference between the interior and the boundary current. Vertically integrating the eddy fluxes, since it is their integral that appears in the buoyancy conservation statements above, and using $\delta\rho(z) = \Delta\rho$ for $-D > z > -h_2$ and 0 elsewhere, one obtains

$$\int_H \overline{u'\rho'}(l, z, t)\, dz = c\Delta\rho\upsilon^* \frac{(D - h_2)^2}{H}, \quad (8)$$

where $D = D(t)$ and $h_2 = h_2(l, t)$.

### e. Model summary

These statements are now combined to yield two coupled equations in two unknowns, $D(t)$ and $h_2(l, t)$. Substituting for the eddy fluxes into (2),

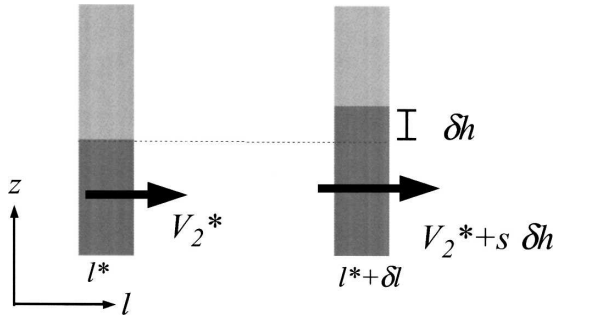


FIG. 3. Schematic of a boundary current water column at $l^*$ and at $l^* + \delta l$. The dense layer thickness has increased by $\delta h$ due to the eddy exchange with the interior. Assuming geostrophy and mass conservation, it follows that the dense layer velocity must increase by $s\delta h$.

$$\frac{dD}{dt} + \frac{Hc}{A\upsilon^*}\int_P V_{\rm bcl}^2\, dl = \frac{dD}{dt} + \frac{\upsilon^* c}{HA}\int_P (D - h_2)^2\, dl = \frac{Q_b}{g'}, \quad (9)$$

where the efficiency coefficient ($c$) is assumed to be constant around the basin.

Consider now (6), the conservation of buoyancy statement for the boundary current, in which the eddy fluxes contribution can be replaced by (8). The divergence term can be expanded as the sum of a term due to changes in the layer thickness $h_2$ and of a term due to changes in the layer velocity $V_2$:

$$\frac{\partial h_2}{\partial t} + V_2\frac{\partial h_2}{\partial l} + h_2\frac{\partial V_2}{\partial l} = \frac{Hc}{\upsilon^* L}V_{\rm bcl}^2 = \frac{\upsilon^* c}{HL}(D - h_2)^2. \quad (10)$$

Using geostrophy and mass conservation, this can be written as

$$\frac{\partial h_2}{\partial t} + V_{\rm adv}\frac{\partial h_2}{\partial l} = \frac{Hc}{\upsilon^* L}V_{\rm bcl}^2, \quad (11)$$

where

$$V_{\rm adv} = V_2 + sh_2 = V_2 + \upsilon^* \frac{h_2(D - h_2 + h_1)}{H^2} \quad (12)$$

is an effective, advective velocity for the dense layer thickness and $s = \partial V_2/\partial h_2$, that is, the rate of change of the dense layer velocity as a function of its thickness. Effectively $s$ accounts for having imposed that the system conserve mass and remains geostrophic. To gain some physical insight into $s$, consider the following steady-state argument (Fig. 3). Let $h_2^*$ and $V_2^*$ be the dense layer thickness and velocity at $l = l^*$ and suppose that at $l = l^* + \delta l$ the dense layer thickness has in-

creased due to eddy fluxes, such that $h_2(l^* + \delta l) = h_2^* + \delta h$, where $\delta h$ is small but positive. Because of the thickness variation, it follows that the baroclinic velocity must have decreased by $v^*\delta h/H$. Using this fact and mass conservation and assuming changes are small, the change in the dense layer velocity is $\Delta V_2 = V_2(l^* + \delta l) - V_2(l^*) = s\delta h$.

Last, because of the assumption that changes in the total water depth ($H$) are small with respect to changes in the layers' thickness, there is no prognostic equation for $H$ or for $V_{\text{btp}}$, and mass conservation can be written as

$$\frac{\partial V_{\text{btp}}}{\partial l} = 0.$$

Parameters that need to be specified for the solution are $H$, $h_2(l = 0)$ (i.e., the thickness of the dense water at inflow), $V_{\text{btp}}$, $\Delta\rho$, $Q_b$, $c$, plus the geometric parameters of the problem. Equations (9) and (11) are then the two nonlinear, coupled model equations in two unknowns $D(t)$ and $h_2(l, t)$. For time-varying problems, the initial values of these two fields must also be supplied.

### f. *Diagnostics: Poleward heat transport, transformation, and overturning*

From the perspective of the large-scale and thermohaline circulations, one is interested in the changes in circulation, buoyancy, or heat content due to convection in the basin. A number of such quantities are defined in this section, mostly relating to the concept of water mass transformation.

One relevant quantity is the net amount of heat (equivalent to buoyancy in the absence of salt) that the boundary current releases to the basin's interior, and eventually to the atmosphere. For simplicity, I refer to this quantity as the net poleward heat transport (PHT), or equivalently (except for the units) to the net poleward buoyancy transport (PBT). Strictly speaking, however, the term poleward implies that one is considering differences in the meridional transport only and, hence, depends on the orientation of the basin. For the purpose of this study, however, the poleward transport is simply intended as the transport change due to convection occurring in the basin. The poleward transport of buoyancy, or heat, at any given point around the basin ($l$) is defined as the difference between the transport at that point minus the transport at inflow (where the transport has been integrated vertically and across-stream):

$$\text{PBT}(l) = g\alpha\text{PHT}(l) = -Lg'\int_0^l \frac{\partial}{\partial l}(V_2h_2)\,dl, \quad (13)$$

where $\alpha$ is the thermal expansion coefficient. As will be shown later, this is a negative quantity since the current is losing buoyancy (heat) around the basin. The net poleward buoyancy transport for the basin is simply given by

$$\text{PBT}(P) = -Lg'(V_2h_2)_{\text{in}}^{\text{out}} = -g'w^*, \quad (14)$$

where $w^*$ is the diapycnal mass flux, that is, a measure of how much excess dense water is leaving the basin relative to that flowing into it at any given time. This will generally not match the rate of dense water formation in the interior at that given instant; picture, for example, a basin in which convection has ceased but excess dense water is still being drained out the basin. In steady state, however, the diapycnal mass flux must equal the amount of fluid transformed:

$$w^* = \frac{Q_bA}{g'}. \quad (15)$$

From (13), the poleward heat transport can be decomposed in two terms:

$$\text{PBT}(l) = -Lg'\left(\int_0^l h_2\frac{\partial V_2}{\partial l}\,dl + \int_0^l V_2\frac{\partial h_2}{\partial l}\,dl\right), \quad (16)$$

one representing the contribution from changes in velocity and a second due to the changes in the vertical structure of the boundary current. Given (4), it is straightforward to see that the first term represents the diapycnal mass flux associated downwelling across the layer interface in the boundary current. Integrating from inflow to outflow, the total diapycnal mass flux can be written as the sum of these two terms:

$$w^* = w_O + w_H = L\left(\int_0^P h_2\frac{\partial V_2}{\partial l}\,dl + \int_0^P V_2\frac{\partial h_2}{\partial l}\,dl\right). \quad (17)$$

This decomposition is physically significant since it shows that the net poleward buoyancy transport is due to two distinct terms. In part, it results from a diapycnal mass flux within the boundary current brought about by the downwelling of fluid across the layer interface. This term will be referred to as the overturning contribution, $w_O$. In part, it is achieved through a horizontal transport term, $w_H$, which can be loosely thought of as horizontally advecting property anomalies around the basin. To visualize why $w_O$ is referred to as the overturning contribution, consider Fig. 4. The sinking in the boundary current is represented through the speeding

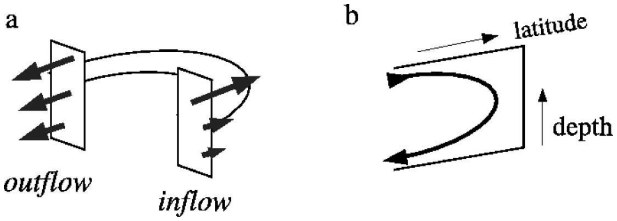


FIG. 4. (a) Downwelling across a surface: if the transport occurring beneath a given surface has increased from inflow to outflow (as shown), it follows that some fluid must have downwelled (sunk) across the surface; (b) overturning circulation: if downwelling has occurred around the boundary current, the zonal average of the circulation across the basin will yield an overturning circulation.

up of the dense layer (Fig. 4a) so that the current becomes more barotropic. The overturning circulation emerges clearly by averaging the flow across the basin (zonally for a meridional inflow/outflow, Fig. 4b), as typically done in ocean circulation numerical models to diagnose the overturning streamfunction. It is effectively a measure of how much fluid is exiting at a depth greater than that at which it came in, and hence of the overturning associated with convection in the basin. It is important to realize that it is distinct from the eddy-induced overturning circulation often loosely associated with convective basins (e.g., Khatiwala and Visbeck 2000), which is not a mean circulation but instead an eddy-driven diapycnal mass flux.

Last, the horizontal term can be further decomposed in a barotropic plus a baroclinic contribution (as has been done in PS06). For the purpose of this study, however, this term is simply referred to as the contribution from the horizontal circulation, $w_H$.

### g. Conditions at inflow

Conditions at inflow that must be specified include the baroclinic structure of the boundary current, that is, $h_0 = h_2^{in} = h_2(l = 0)$, the total barotropic transport $V_{\text{btp}}$, and one more velocity condition. It is assumed that the flow around the basin is due both to the convection occurring within the basin (buoyancy driven) and to remote forcing (e.g., by wind). For simplicity, the remotely driven circulation, $V^W$, is assumed to be barotropic and is imposed as an external parameter at inflow. For the buoyancy driven circulation, the isopycnal slope between the interior and the boundary current only constrains the baroclinic shear (i.e., $V_{\text{bcl}}$), leaving the barotropic transport associated with the buoyancy driven circulation, $V^B$, unspecified. For clarity, a parameter $\eta$ is introduced to define the fraction of the inflow baroclinic velocity ($V^0_{\text{bcl}}$) found in the light layer at inflow ($l = 0$):

$$\left.\begin{aligned} V_1^0 &= V^W + \eta V_{\text{bcl}}^0 \\ V_2^0 &= V^W + (\eta - 1)V_{\text{bcl}}^0 \end{aligned}\right\} \Rightarrow V_{\text{btp}} = V^W + V^B = V^W + V_{\text{bcl}}^0(\eta H - h^0)/H.$$

Some guidance on the magnitude (and sign) of the buoyancy-driven transport can be found in the simulations of convection in a circular, semienclosed basin both with and without topography of Spall (2004, 2003), respectively. Flat bottom simulations had a zero, vertically integrated transport, to be contrasted with those in the presence of topography where there exists a nonzero buoyancy-driven net transport.

Throughout this study, it is assumed that $\eta = 1$; that is, all of the buoyancy-driven flow is initially concentrated in the light layer. An exception is made for the Labrador Sea case presented below where the inflow velocity for the dense layer is actually taken from data. For all other cases, however, note that this choice of $\eta = 1$ does not modify the structure of the solution but only shifts it in terms of absolute transport.

## 4. Validity of the model for the Labrador Sea

Given the model described above, it is legitimate to ask to what it extent it can reproduce the gross, observed features of dense water formation in the Labrador Sea. After briefly explaining how model parameters were selected to fit observations from the region, three model runs are discussed and compared to observations: steady state, seasonal cycle, and shutdown of convection.

### a. Parameters

The Labrador Sea interior is assumed to be a cylinder of radius $R = 230$ km, while the boundary current is characterized by a perimeter $P = 2000$ km and a width $L = 100$ km (see the late spring climatological, averaged from 1990 to 1997, hydrographic section across the basin in Fig. 5; this is the same data described by PS06). Following Straneo (2006), $\sigma_\theta = 27.72$ is chosen as the isopycnal roughly separating the light layer from the dense layer. The total depth $H$ of the two layers is set to 1500 m, which corresponds to the base of LSW in the boundary current (i.e., to $\sigma_\theta = 27.78$, Fig. 5) and, hence, to the combined thickness of the light and

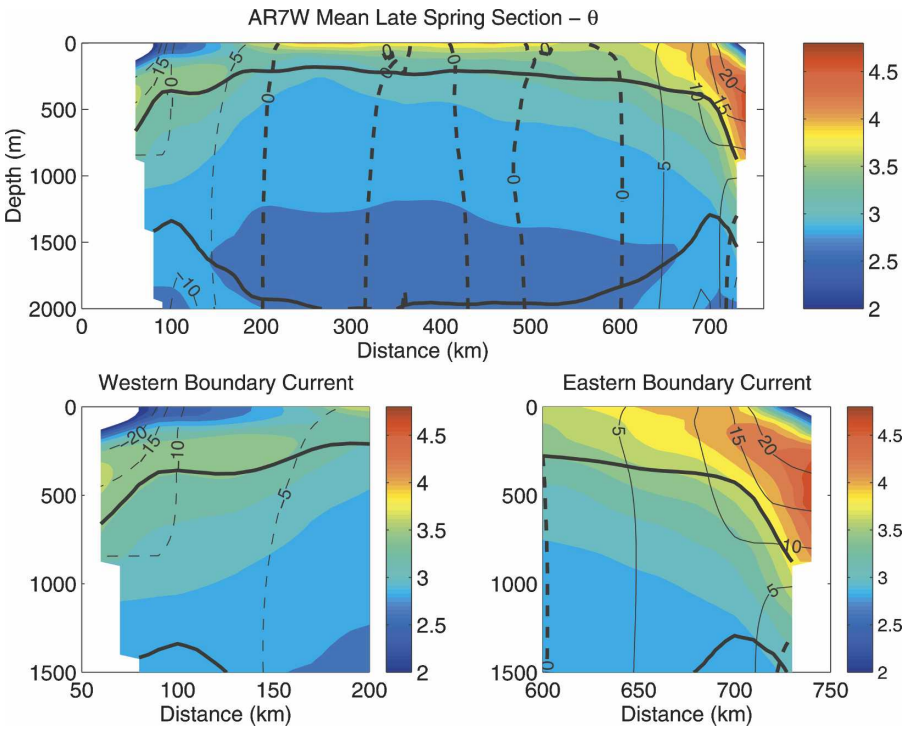


FIG. 5. (a) Potential temperature section across the Labrador Sea (section AR7W) from PS06. Two isopycnals, 27.72 $\sigma_\theta$ and 27.78 $\sigma_\theta$, are overlaid as thick black, solid lines. Velocity contours are shown as thin vertical lines (dashed is out, solid is in, and zero is thick dashed); (b) inflowing boundary current enlarged; (c) outflowing current enlarged.

dense layers in the boundary current.[4] The other model parameters are derived from the section shown in Fig. 5: $h_0 = 700$ m, and $V_2(l = 0) = 0.08$ cm s$^{-1}$, $\Delta\rho = 0.05$ kg m$^{-3}$. For the steady-state simulations, the surface cooling is set to 25W m$^{-2}$ [i.e., the mean net annual loss equally distributed throughout one year, see Straneo (2006), for a discussion of the climatological surface forcing]. In the seasonal simulations, the same net surface heat loss is concentrated over a four-month period (January–April). Given this choice of parameters, the rate of formation of LSW from (15) is approximately 2 Sv. This is within the observed range as described by Clarke and Gascard (1983) or Smethie and Fine (2001). It is not inconsistent with larger estimates of LSW formation ranging from 1.2 to 11 Sv (Rhein et al. 2002) if one takes into account that this only reflects the amount of LSW formed within the central Labrador Sea. Khatiwala et al. (2002) estimated similar rates using several climatological datasets. Last, $c$ is set to 0.03 within the range of the empirically derived values (see Jones and Marshall 1997; Spall and Chapman 1998).

### b. Steady-state solution

In steady state, a constant rate of LSW formation in the interior must be balanced by its removal by the boundary current, and the diapycnal mass flux (15) is exactly equal to the amount of dense water formed. While one expects the dense layer thickness in the boundary current to increase around the basin, a priori one does not know how the increase is distributed along the entire perimeter. The baroclinic shear must also decrease around the basin (since the interior/boundary current isopycnal slope decreases), which will impact the velocity around the basin and hence potentially affect the solution.

The steady-state equations, using Labrador Sea parameters, are solved using a finite-difference fourth-order Runge–Kutta scheme for the boundary current thickness equation, while iteratively satisfying the constraint for the interior dense layer thickness. From

[4] Note that the total layer thickness in the interior is larger because of the presence of the Nordic seas overflow waters (larger thickness in the boundary current than in the Labrador Sea interior). Because the overflow is not thought to play an active role in LSW formation, however, the total interior thickness is also set to 1500 m.

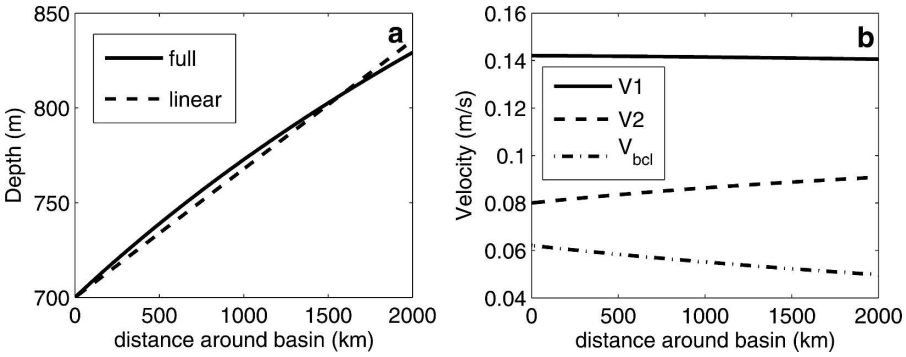


FIG. 6. Steady-state solution for the Labrador Sea case: (a) dense layer thickness change around the perimeter. Solid is the full numerical solution and dashed is the linear solution discussed below; (b) velocities around the basin.

these we obtain the equilibrium value for $D$, the dense layer thickness in the interior, and for $h_2(l)$, the dense layer thickness around the boundary current, and can then use geostrophy and mass conservation to obtain $V_1$ and $V_2$.

The steady-state solution for the Labrador Sea case is shown in Fig. 6. As expected, the dense layer thickness increases (at a mostly uniform rate) around the basin for a net thickness change of about 130 m from inflow to outflow (Fig. 6a). The equilibrium LSW thickness in the interior, from the model solution, is of 1350 m. Also shown are the changes in the velocities (Fig. 6b). Given the reduction in thickness gradient between the interior and the boundary current around the basin, it follows that the baroclinic flow must also decrease. This, combined with mass conservation, implies that the dense layer must speed up. One can think of this as a redistribution of momentum associated with the imposed geostrophy and mass conservation. If the dense layer speeds up, it follows that some fluid has to sink. To see this consider Fig. 4b, and let the horizontal surface be that corresponding to the layers' interface at inflow. Fluid beneath this layer consists of only dense fluid (from inflow to outflow); hence if the dense waters are moving faster, it follows that the transport out beneath this layer is greater than the transport in; that is, some fluid has crossed this interface. Note that the light layer velocity also changes (decreases) but the change is small.

The relative contribution to the net poleward buoyancy transport of the horizontal and overturning circulations can be estimated using (17). For the Labrador Sea case, it is estimated that 1.2 Sv (60%) of the transport is achieved by the horizontal circulation, compared to 0.8 Sv (40%) by the overturning circulation.

These numbers are compared to observations as follows. The light layer thickness in the interior deduced from the model is comparable to that thickness of a layer bound by the surface and $\sigma_\theta = 27.72$ (Straneo 2006) although perhaps somewhat on the thin end. The net thickness change in the boundary current is compared to that shown in Figs. 5b and 5c. The mean thickness of the light layer at inflow (at the eastern boundary) is estimated by averaging the thickness of the layer bound by the surface and $\sigma_\theta = 27.72$, across the approximately 100-km boundary current, and similarly for outflow (western boundary). This yields a mean thickness of 570 m at inflow, compared to a thickness at outflow of 450 m (Figs. 5b and 5c), and hence a thickness change of 120 m, which is of the same order of magnitude as the model prediction. The same result can be obtained by calculating the change in the dense layer whether one uses a fixed depth (1500 m) as the lower boundary or a dense isopycnal such as $\sigma_\theta = 27.78$. PS06 used climatological late-spring hydrographic data combined with the absolute velocity field measured by Profiling Autonomous Lagrangian Current Explorer (PALACE) floats, and estimate a sinking of approximately 1 Sv from intermediate to dense water, which compares favorably to the 0.8 Sv obtained in this model. Also comparable with their results is a transport of approximately 12 Sv in the light layer and of 5–6 Sv in the LSW. So, overall, it appears that this simple model is able to reproduce the basic features of the system. It should be clear, nonetheless, that this comparison is only meant in qualitative sense since the section represents mean spring conditions and not a true annual average.

### c. Seasonal cycle

The seasonal cycle is simulated by integrating the full time-dependent equations and forcing the system with a buoyancy loss that is concentrated over the winter months (Fig. 7a). The system is initialized with the steady-state solution. Then the dense layer thickness in

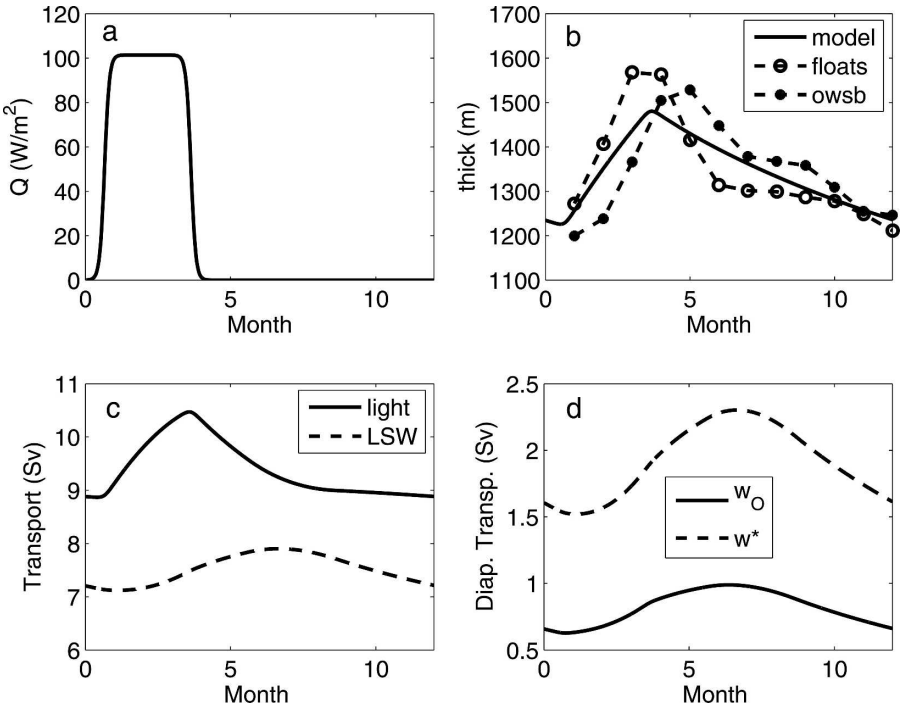


FIG. 7. Seasonal model cycle for the Labrador Sea: (a) net surface forcing; (b) thickness of the dense layer in the interior from model, float data (1996–2000), and Ocean Weather Station Bravo data (1964–74); (c) transport at outflow for the two layers; (d) total ($w^*$) and overturning ($w_O$) diapycnal mass fluxes from (17).

the interior is forward stepped in time, using the prescribed surface forcing and the boundary current structure at the earlier time step (to calculate the eddy fluxes). Once the interior thickness value is obtained, the boundary current solution is time-stepped (again using a forward difference scheme) according to (11). A weak Laplacian diffusion is added to (11) for numerical stability purposes. The time step used is 6 h. It takes the model approximately 4 years to spin up to a stable seasonal cycle, after this it is run for another 10 years (total 15). The solution presented is for the last year of integration.

During the winter months light water is converted into dense water causing the layer interface in the interior to rise. This rise is contrasted by the action, throughout the entire year, of the eddy fluxes acting to remove the gradient between the interior and the boundary current. The seasonal pattern that results, in the interior, is one with a rapid rise in dense layer thickness during the winter and a slow decay for the rest of the year (Fig. 7b). This pattern is similar to that described in a number of data analysis studies for the annual cycle of LSW thickness (Khatiwala et al. 2002; Lilly et al. 2003; Straneo 2006). Here, it is compared with the mean motion of the $\sigma_\theta = 27.72$ from the Ocean Weather Station Bravo data from 1964 to 1974 (excluding the years when convection was shut down: 1969–1971) and with that observed by PALACE floats for the period from 1996 to 2000 [see Straneo (2006), for a detailed description of the data]. It is not surprising that the model prediction has a slightly reduced amplitude since it reflects conditions averaged over the Labrador Sea interior, while the data are biased toward the region of deepest convection.

The seasonal cycles of the layer transports are shown in Fig. 7c. The total (barotropic) transport has a seasonal variation of approximately 2 Sv. This arises from allowing conditions within the basin to "rule" the inflow; specifically an increased LSW thickness during the winter will increase the net flow of light water into the basin and hence the total transport. The LSW transport out of the basin, on the other hand, peaks sometime in the summer with a delay of several months with respect to the maximum thickness of LSW in the interior. This delay reflects the slowness in the exchange between the interior and the boundary current and the progressive accumulation of LSW in the boundary current as it travels around the basin. This same lag at outflow is seen in the overturning and total diapycnal mass fluxes (Fig. 7d). There are currently no observations of the seasonal variation in transport to support, or dispute, the model's prediction and, as pointed out

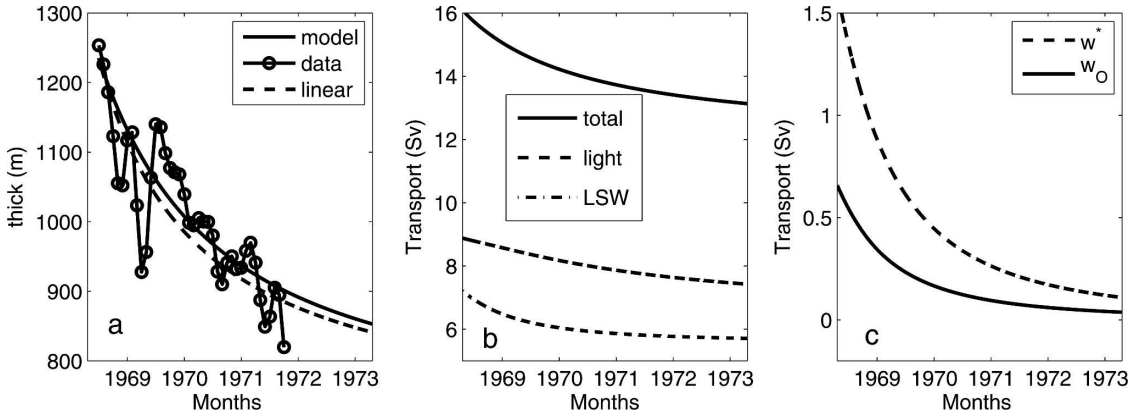


FIG. 8. Shutdown of convection simulation: (a) thickness of the dense layer in the interior from the model and from the OWS Bravo data (1969 to 1972). Also shown is the linear model prediction described in section 5; (b) transport at outflow; (c) total and overturning diapycnal mass fluxes as in (17).

by one reviewer, a 2-Sv seasonal variation in a 20-Sv transport (over the light and dense layers) is relatively small and likely in the noise level.

### *d. Shutdown of convection*

A second, relevant time-dependent problem is the evolution of the system in the absence of convection (due, e.g., to weak surface forcing or to a freshwater anomaly). In this simulation the fields are initialized with the end-of-the-year conditions from the seasonal cycle described above and allowed to evolve with no surface forcing applied. The cessation of LSW renewal causes, predictably, a decrease in the thickness of LSW water in the interior (Fig. 8a). (If allowed to evolve indefinitely, the thickness tends to that specified at inflow such that the eddy fluxes tend to zero.) The drop in LSW is compared with that observed from 1969 to 1971 in the Labrador Sea when convection was limited to 200 m (i.e., to the surface layer; Lazier 1980). Shown in Fig. 8b is the drop in the $\sigma_\theta = 27.72$ isopycnal during that period. Notwithstanding the variability in the data, the agreement between the model and data is quite good.

Associated to a shrinking of the LSW layer in the interior, there occurs a decrease in the total transport out of the basin (due to decrease in the transport into the basin) as well as decrease in the transport of LSW out of the basin (Fig. 8b). Similarly, there occurs a decrease in the overturning and total diapycnal mass fluxes (Fig. 8c). As for the seasonal cycle, there are no observations for comparison.

## 5. Theory: The steady-state problem

### *a. Preliminary considerations*

Some insight into the dynamics described by the model equations can be gained from some basic considerations. As the source region for the dense water, the interior will generally have a thicker dense layer than the boundary current. An exchange between these two regions will therefore cause the dense layer thickness in the boundary current to increase around the basin; that is, $\partial h_2/\partial l > 0$. As a result, the baroclinic velocity must decrease around the basin and, because of this, the velocity of the dense layer must increase:

$$\frac{\partial V_2}{\partial l} = \frac{V_{\rm bcl}}{H}\frac{\partial h_2}{\partial l} - \frac{h_1}{H}\frac{\partial V_{\rm bcl}}{\partial l} > 0.$$

It follows, then, that the transport of dense water will increase both as a result of the increase in thickness and also from a speeding up of this layer. If the dense layer accelerates around the basin, it follows that some sinking must occur in the boundary current since more fluid is exiting between the bottom and $h_2(l = 0)$ than entered [Fig. 4 and (4)]. While the details of this sinking are not explicitly resolved by this model, it arises as a consequence of having imposed that, as the interior/boundary current thickness gradient decreases around the boundary, the flow remains geostrophic and conserves mass.

Note that, while the transport of light fluid around the basin must necessarily decrease to balance the increase in dense fluid transport, no a priori statement can be made about the change in velocity of the light layer. From the definition of $V_1$, one can readily show that

$$\frac{\partial V_1}{\partial l} = \frac{v^*}{H^2}\frac{\partial h_2}{\partial l}(D - 2h_2),$$

which is less than zero only if $h_2 > D/2$. While this is true for the Labrador Sea case discussed above, this need not be necessarily always the case. As pointed out

by one reviewer, for the extreme case when $D > 2h_2$, that is, the interior dense layer is very thick relative to the dense layer thickness in the boundary current, $V_1$ would actually increase around the basin. This would imply the existence of an upper upwelling cell that would partially offset the downwelling occurring deeper in the water column.

*b. Linear solution*

There are two nonlinear terms in the model equations: the eddy flux contribution, appearing both in the interior and boundary current buoyancy conservation statements, and the divergence term, found in the latter only, which make it difficult to find an exact solution to the problem. A general understanding of the physics of the system, however, can be gained by assuming that changes in the layer thicknesses around the basin are small and by solving for the linearized system. Let $h_2(l) = h_0 + h'(l)$ and $V_{\rm bcl} = V^0_{\rm bcl} - \upsilon^* h'/H$. Conditions on $h'$, such that both nonlinear terms can be reduced to linear terms, are: $h' \ll D - h_0$ for the eddy flux term and $h' \ll h_0$ for the advection term. Assuming that both of these conditions are met, then the equations can be linearized about the inflow values, denoted by a 0 superscript or subscript. Let $D_0 = D - h_0$ be the boundary current/interior gradient at inflow and neglecting terms of order $h'^2$, the linearized system can be written as

$$\frac{\partial h'}{\partial l} = \frac{\gamma}{P}(D_0 - 2h') \quad \text{and} \tag{18}$$

$$D_0\left[PD_0 - 2\int_P h'(l)\,dl\right] = \frac{Hw^*}{c\upsilon^*}, \tag{19}$$

where

$$\gamma = \frac{V^0_{\rm bcl}}{V^0_{\rm adv}}\frac{cP}{L} = \beta\epsilon$$

is the product of two terms, both potentially small. The first, $\beta$, is the ratio of the baroclinic velocity at inflow to the effective advective velocity for the dense layer. If the wind-driven circulation is zero, this term is roughly of $O(1)$. The second term, $\epsilon$, on the other hand, represents a measure of the eddy efficiency. The product of these two terms, $\gamma$, is the ratio of the fluid exchanged by the eddies to the fluid circulating around the basin. As long as this number is small, the solution is mostly linear. For comparison, in his scaling analysis Spall (2004) assumed that the magnitude of the advective velocity was comparable to the baroclinic velocity (i.e., $\beta \approx 1$) so that, in that case, $\epsilon$ is the small parameter of the problem.

Using $h'(0) = 0$, the linearized thickness equation can be solved and

$$h'(l) = \frac{D_0}{2}(1 - e^{-2\gamma l/P}). \tag{20}$$

The solution decays exponentially to $D_0/2$ (i.e., to a situation when the eddy fluxes are zero since there is no interior/boundary current gradient). Using (20) and integrating the integral constraint for the interior, one gets

$$h'(P) = \Delta h = \frac{D_0}{2}(1 - e^{-2\gamma}) = \frac{w^*}{LV^0_{\rm adv}}. \tag{21}$$

To first order, then, the net thickness change around the basin is simply given by the ratio of the amount of dense water formed to the transport (per unit height) by the effective advective velocity. It should be noted, however, that $V^0_{\rm adv}$ contains the initial baroclinic velocity, which in turn depends on $D$, the interior dense layer thickness, which is part of the solution. A full solution, which includes an explicit analytic solution for $D_0$, can only be obtained for $\gamma \ll 1$.

For this case,

$$D_0^2 \approx \frac{w^* H}{\upsilon^* L\epsilon},$$

which is equivalent to the solution of Spall (2004) for the interior, and

$$h' = \frac{D_0\gamma}{P}l = \frac{w^*}{LV^0_{\rm adv}}\frac{l}{P}, \quad \text{and}$$
$$V^0_{\rm adv} = V^W + \frac{\upsilon^* h_0}{H^2}(D_0 + H - h_0). \tag{22}$$

In writing (22), I have assumed (as described in section 3f) that $V^0_2 = V^W$; that is, at inflow the flow of the dense layer is due to the remote forcing alone. This assumption simply reduces the complexity of the solution without modifying its character substantially.

Using the linearized expression for $\Delta h$, the horizontal and overturning contributions to the poleward buoyancy transport can be written in terms of conditions at inflow:

$$w^* = w_H + w_O = LV^0_2\Delta h + Ls_0h^0_2\Delta h$$
$$= \frac{V^0_2}{V^0_{\rm adv}}w^* + \frac{s_0h^0_2}{V^0_{\rm adv}}w^*.$$

The ratio of the poleward buoyancy transport achieved by the overturning circulation to that of the horizontal circulation is given by

$$\frac{w_O}{w_H} = \frac{s_0 h_2^0}{V_2^0},$$

which when combined with (22) yields

$$\frac{w_O}{w_H} = \frac{V_{\rm bcl}^0 + \upsilon^*(H - h_0)/H}{V^W} \approx \frac{\left(\dfrac{w^* H}{\epsilon H L}\right)^{1/2} + \dfrac{\upsilon^*(H - h_0)}{H}}{V^W}. \quad (23)$$

While limited in its applicability, the linear solution provides us with some physical insight on the parameters that govern the solution. The thickness variation around the basin (21), in the linear case, is given by the ratio of the amount of water transformed ($w^*$) and the effective mean transport within the dense layer, $V_{\rm adv}^0$. If $w^*$ is fixed, then the thickness change is controlled by changes in $V_{\rm adv}^0$.

One parameter that strongly affects $V_{\rm adv}^0$, and hence $\Delta h$, is the strength of the remotely forced circulation, $V^W$: an increase (decrease) in $V^W$ will lead to a decrease (increase) in $\Delta h$. Physically, this can be understood by considering that a speeding up of the circulation around the basin will give eddies less time to act per unit length of the boundary current: in the extreme of a strong remotely forced circulation, the thickness change will tend to zero. Related to this, the nonlinearity parameter $\gamma$ is also highly sensitive (through $\beta$) to the remotely forced circulation. The fraction of poleward buoyancy transport carried by the horizontal versus overturning circulations is also sensitive to changes in $V^W$. Specifically, if the flow around the basin speeds up, the amount of sinking will decrease leading to a decrease in the overturning circulation.

However, $V_{\rm adv}^0$ is also susceptible to changes in the baroclinic flow and, in particular, to the equilibrium solution for the interior dense layer thickness. An increase in the eddy efficiency, $\epsilon$, will tend to decrease the thickness gradient between the interior and the boundary current, leading to a reduction in the buoyancy driven flow, and hence in $V_{\rm adv}^0$. In turn, this will lead to a larger $\Delta h$, that is, more substantial change in the boundary current and growing importance of the nonlinear terms ($\gamma$ increases). The fraction of PBT due to the overturning circulation will, for growing $\epsilon$, decrease.

An increase in the net buoyancy loss over the basin, $w^*$, will increase the reservoir of dense fluid, thus increasing the thickness gradient, and the fraction of transport carried by the overturning. This is in agreement with the results of many general circulation models that show how an increase in the convective activity will, in general, give rise to an increase in the overturning. These results, however, highlight that this relation is by no means simple.

### c. How linear is the Labrador Sea case?

From the comparison of the full numerical to the linear system's solution shown in Fig. 6a, it is apparent that the Labrador Sea fits the linear regime. In other words, it is a basin where the amount of fluid exchanged by the eddies (to balance the surface buoyancy loss) is relatively small with respect to the transport around the basin. Specifically, evaluation of the nondimensional parameters, for the Labrador Sea parameter choice yields $\epsilon = 0.6$, $\beta = 0.5$, and hence $\gamma = 0.3$.

A quantity of interest, because it reflects the "memory" of the basin, is the flushing time scale for dense water from the interior. The flushing rate, due to the eddies, varies as a function of the gradient between the boundary current and interior, and hence as a function of time. If convection is brought to a halt and if the basin is in a linear regime, however, an approximate flushing time scale can be derived as follows.

By approximating (9) for small changes in the boundary current, one has

$$\frac{dD_0}{dt} = -\frac{\upsilon^* L \epsilon}{AH} D_0(t)^2,$$

whose solution is

$$D_0(t) = D^0\left(1 + \frac{t}{T_f}\right)^{-1}, \quad \text{where} \quad T_f = \frac{AH}{\upsilon^* L \epsilon D^0} = \frac{A}{\epsilon L V_{\rm bcl}^0} \quad (24)$$

and $D^0 = D_0(0)$ is the initial dense layer thickness in the interior. The flushing time is thus given by the volume of interior fluid divided by the rate at which the eddies are exchanging it. For the Labrador Sea case discussed above, the flushing time scale $T_f$ is on the order of 2–3 yr. As shown in Fig. 8a, there is good agreement between the linear and the full numerical solution for the "shutdown of convection" simulation.

### d. Nonlinear numerical solutions

For remotely forced circulations comparable to the buoyancy driven one and for relatively high eddy efficiency, the nonlinear terms become progressively more important. These terms enter the solution when the changes in thickness around the basin have a sizable impact on the velocity field (by modifying the baroclinic shear) so that the coupling of thickness and ve-

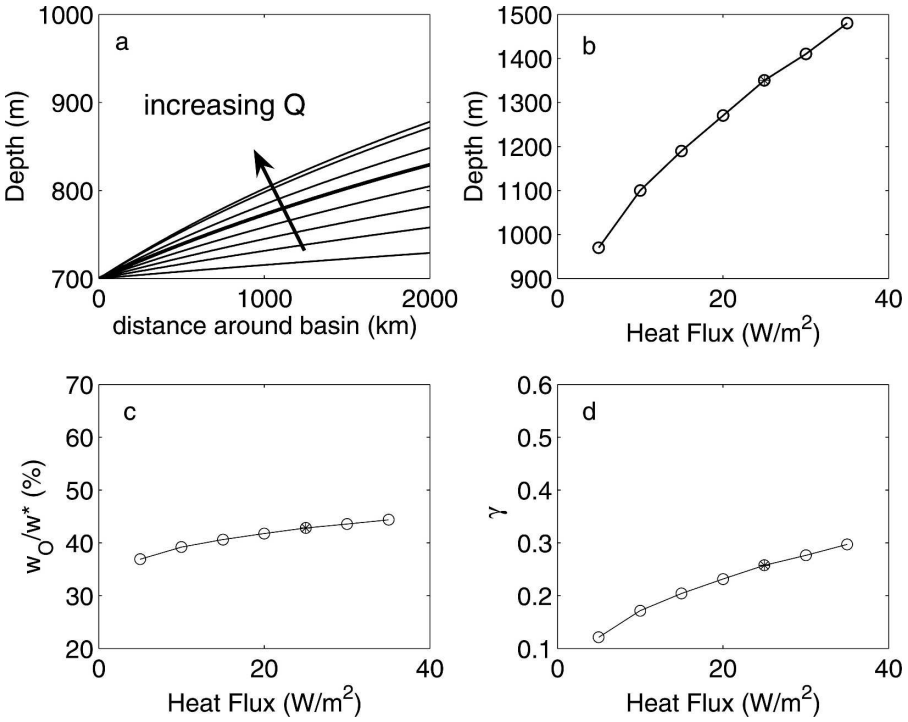


FIG. 9. Sensitivity of the steady-state solution to changes in the surface heat flux $Q$. The Labrador Sea case is shown as a thicker black line or filled circle in all the plots: (a) dense layer thickness around the basin for different values of $Q$; (b) dense layer thickness in the interior; (c) fraction of the poleward buoyancy transport carried by the overturning circulation; (d) nonlinearity parameter $\gamma$.

locity changes impacts the solution. No explicit solution is presented for the nonlinear regime. Instead a series of numerical solutions for the steady-state problem using a range of $V^W$ and $Q$ are used to explain the impact of the nonlinear terms (Figs. 9 and 10). As for the linear case, an increase in the net buoyancy loss will lead to a larger reservoir of LSW in the basin's interior (Fig. 9b). An increased interior/boundary current gradient (at least at inflow) will, in turn, lead to an increase in the eddy fluxes and thus to a more significant modification of the boundary current. Thus, solutions progressively deviate from the linear solution (Fig. 9a). As the solution becomes progressively more nonlinear (Fig. 9d), the boundary current loses more buoyancy upon entering the basin and less while exiting (to be contrasted with the linear solution where buoyancy loss occurs at constant rate). This reflects how the eddy fluxes, through the alteration of the baroclinic structure, affect the flow around the basin, which in turn feeds back on the eddy fluxes. Last, as the solution becomes more nonlinear and $\Delta h$ larger, the fraction of PBT carried by the overturning circulation increases by a small amount from 35% to 40% (Fig. 9c).

In general, as discussed for the linear case, an increase in the barotropic circulation around the basin will lead to a decrease in the changes in the boundary current, and hence to a decrease in the relevance of the nonlinear terms (Fig. 10a). The impact of $V^W$ on the interior thickness is limited and can be explained by considering that the layers' interface slope from inflow to outflow decreases with increasing $V^W$ so that the eddy fluxes effectively increase the buoyancy transport into the interior (Fig. 10b). The impact on the role of the overturning circulation in the PBT is, on the other hand, very large. In weak wind regimes, with basins dominated by the buoyancy-driven circulation, most of the PBT is achieved by the overturning circulation. On the contrary, basins characterized by a large remotely forced circulation tend to carry most of the PBT via the horizontal circulation terms, Fig. 10c. Similarly, $V^W$ has a large impact on the degree of linearity of the solution (Fig. 10d).

## 6. Summary

An idealized, two-layer, isopycnal model for a semienclosed convective basin is proposed in this study. The model consists of an interior, horizontally homo-

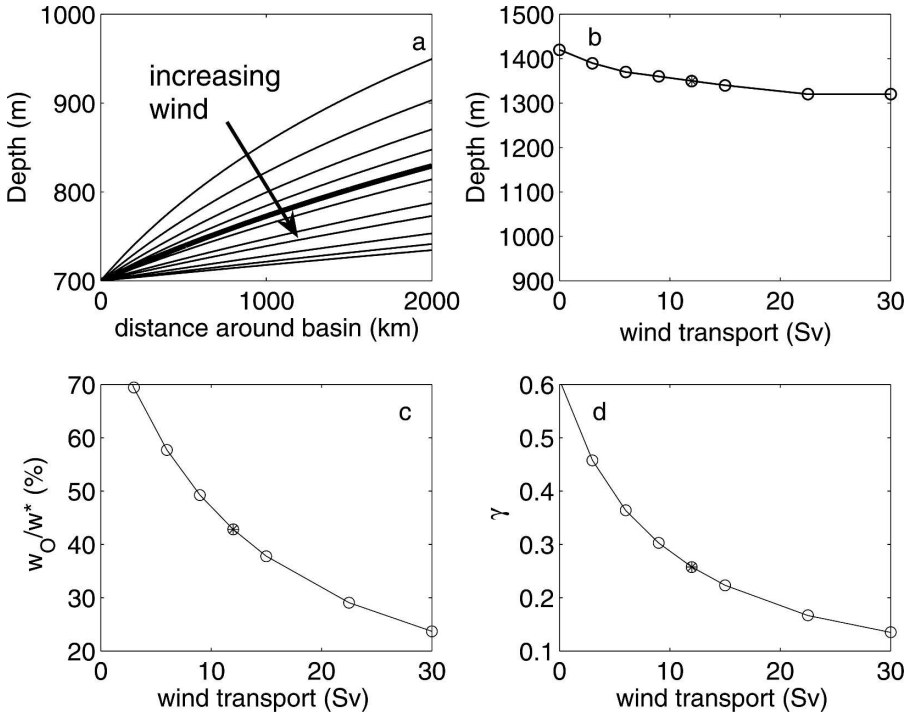


FIG. 10. As in Fig. 9 but for changes in $V^W$, the remotely forced circulation.

geneous, region and a surrounding boundary current. A large surface buoyancy loss drives convection in the interior region, which in the model is represented as a transformation of light fluid into dense fluid. The boundary current is the means by which light fluid is advected into the basin and dense fluid removed. Flow around the basin is due both to remote forcing (e.g., wind) and to the buoyancy forcing that sets up the interior/boundary current gradients, and it is assumed to be in geostrophic balance. The exchange between the boundary current and the interior is due to eddies, which are included in the model in parameterized form. The model formulation is supported (and suggested) by a number of recent observational and modeling studies of the Labrador Sea.

Numerical solutions for a realistic Labrador Sea case study are obtained for three different forcing regimes: steady state (uniform buoyancy loss), seasonal (buoyancy loss in the winter only), and shutdown of convection (zero buoyancy loss). In all three cases the model results compare favorably to the existing observations. Furthermore, the model makes a number of predictions that supplement the existing data. For the Labrador Sea case, the model predicts that the increase in the dense water in the boundary current occurs at a mostly uniform rate. Also, it shows how the net poleward transport of buoyancy (or equivalently heat) is carried out to a larger extent by the horizontal circulation (60%) and to a lesser extent by the overturning or vertical circulation (40%). In the seasonally forced simulation, the model predicts that the maximum transport in Labrador seawater out of the basin occurs with a 3–4-month delay with respect to the maximum convection in the interior. This delay is dictated by the rate at which the eddies are able to remove the excess dense water from the basin. The flushing time for the basin is estimated to be on the order of 2–3 yr.

Analysis of the steady state, linearized model equations provides further insight into the dynamics at play. The degree of linearity of the problem is determined by the ratio of the fluid exchanged by the eddies to the fluid that circulates around the basin. If this ratio is small, the changes in the boundary current structure are small. The Labrador Sea is in this regime owing to both the limited efficiency of the eddy fluxes and to the large barotropic transport around the basin. In the linear regime, changes in the velocity structure of the boundary current do not significantly affect the buoyancy exchange between the interior and the boundary current; hence this occurs at a uniform rate. In the nonlinear regime, the bulk of the transfer of buoyancy occurs early on (meaning close to inflow) as the impact of the buoyancy loss is to decelerate the light water, which in turn allows the eddies more time to extract the buoyancy. The increase in the remotely forced circulation, a decrease in the eddy efficiency, or in the net buoyancy

removed from the interior, tend to result in a more linear solution.

One important result of this work regards the concept of overturning circulation. While its details are not resolved explicitly in this model, how much sinking has to occur and its timing can be diagnosed from the boundary current solution. In particular, the dynamics described by the model's equations show that sinking in the boundary current has to occur as a result of changes in the current's baroclinic structure. This downwelling, when horizontally averaged across the basin, gives rise to an overturning circulation in depth space. Physically, it is dictated by geostrophy and mass conservation: as the thickness interface slopes, the dense layer is accelerated around the basin and some fluid has to sink to conserve mass.

Both the linear analysis and the numerical solutions show that both the magnitude of the downwelling and its role in the poleward buoyancy transport can vary even if the amount of dense water formed in the basin is maintained constant. This result highlights the importance of distinguishing between water mass transformation and overturning, that is, between the PBT and the MOC (often taken to be covarying). For example, it is shown that, if the remotely forced circulation (e.g., by wind) increases, the overturning will decrease, even for the same amount of dense water formed. Also, it is shown that the ratio of poleward buoyancy transport by the horizontal versus the overturning circulation is not an intrinsic property of a basin but that it will change with changes in the circulation, the eddy efficiency, and the net buoyancy loss.

## 7. Discussion

The model presented in this study is primarily intended as a tool with which to investigate the connection between the thermohaline circulation and those regions that are presumed to be part of its driving force, that is, the convective regions. Its usefulness lies mostly in providing simple, explicit ways with which to relate quantities such as the transport around the basin, the transformation of the boundary current, and the horizontal and overturning circulation. Its applicability is not limited to the Labrador Sea alone since there are no special features that set this basin apart from other convective basin. Clearly though, features such as sea ice, sills, or more than one open boundary may add layers of complexity to the problem.

To keep the model dynamics as simple as possible, I have made a number of simplifications. Three that may seem questionable are 1) there is no convection in the boundary current, 2) the convective basin/external ocean exchange is limited to what is carried in and out by the boundary current, and 3) the effects of freshwater are not included. While all three potentially play a role in dense water formation in the Labrador Sea, I believe that they are not the dominant players and that, to first order, the basic dynamics is well represented by the system.

A number of other assumptions have been made with regards to conditions at inflow. First, the boundary current structure at inflow is assumed to be set by conditions outside of the basin and is held constant. Presumably though, there will be a feedback between what happens in the basin and the baroclinic structure at inflow on long time scales. This feedback is not included in the discussion. Second, the net transport associated with the buoyancy-driven circulation remains an open question. Third, potential feedbacks between the amount of heat lost in the convective basin with the water inflow characteristics or, for example, the large-scale wind field have not been considered here.

Notwithstanding all the simplifications, I believe that the model is a useful tool for the understanding of the connection between convective regions and the thermohaline circulation, and their respective variabilities. It may also serve as a useful tool for the interpretation of data or general circulation models. It shows clearly how quantities such as overturning and water mass transformation are not trivially related and must not be taken as synonyms.

Of relevance to the large-scale oceanic circulation, this model highlights the role of the wind-driven circulation in affecting the net sinking of dense water in a convective basin: a faster remotely forced circulation implies less sinking for the same amount of dense water formed. This raises some issues as to the possibility of treating convective regions simply as sinking regions and, in general, of decoupling the wind-driven circulation from the buoyancy-driven one.

*Acknowledgments.* The author is greatly indebted to Mike Spall and Bob Pickart for many insightful discussions and for use of the hydrographic climatological section data. This work was supported by NSF OCE 02-40978 and by the Climate Institute at the Woods Hole Oceanographic Institution (WHOI).

REFERENCES

Bentsen, M., H. Drange, T. Furevik, and T. Zhou, 2004: Simulated variability of the Atlantic meridional overturning circulation. *Climate Dyn.,* **22,** 701–720.

Brandt, P., F. Schott, A. Funk, and C. Sena Martins, 2004: Seasonal to interannual variability of the eddy field in the Labrador Sea from satellite altimetry. *J. Geophys. Res.,* **109,** C02028, doi:10.1029/2002JC001551.

Clarke, R. A., and J. C. Gascard, 1983: The formation of Labrador Sea Water. Part I: Large-scale processes. *J. Phys. Oceanogr.,* **13,** 1764–1778.

Cuny, J., P. Rhines, P. Niiler, and S. Bacon, 2002: Labrador Sea boundary currents and the fate of Irminger Water. *J. Phys. Oceanogr.,* **32,** 627–647.

Eden, C., and J. Willebrand, 2001: Mechanism of interannual to decadal variability of the North Atlantic Circulation. *J. Climate,* **14,** 2266–2280.

——, and C. Böning, 2002: Sources of eddy kinetic energy in the Labrador Sea. *J. Phys. Oceanogr.,* **32,** 3346–3375.

Jones, H., and J. Marshall, 1993: Convection with rotation in a neutral ocean: A study of open-ocean deep convection. *J. Phys. Oceanogr.,* **23,** 1009–1039.

——, and ——, 1997: Restratification after deep convection. *J. Phys. Oceanogr.,* **27,** 2276–2287.

Katsman, C. A., M. A. Spall, and R. S. Pickart, 2004: Boundary current eddies and their role in the restratification of the Labrador Sea. *J. Phys. Oceanogr.,* **34,** 1967–1983.

Khatiwala, S., and M. Visbeck, 2000: An estimate of the eddy-induced circulation in the Labrador Sea. *Geophys. Res. Lett.,* **27,** 2277–2280.

——, P. Schlosser, and M. Visbeck, 2002: Rates and mechanisms of water mass transformation in the Labrador Sea as inferred from tracer observations. *J. Phys. Oceanogr.,* **32,** 666–686.

Lab Sea Group, 1998: The Labrador Sea Deep Convection Experiment. *Bull. Amer. Meteor. Soc.,* **79,** 2033–2058.

Lavender, K., R. E. Davis, and W. B. Owens, 2000: Mid-depth recirculation observed in the interior Labrador and Irminger Seas by direct velocity measurements. *Nature,* **407,** 66–99.

Lazier, J. R. N., 1980: Oceanographic conditions at Ocean Weather Ship Bravo, 1964–1974. *Atmos.–Ocean,* **18,** 227–238.

——, and D. G. Wright, 1993: Annual velocity variations in the Labrador Current. *J. Phys. Oceanogr.,* **23,** 659–678.

——, R. Hendry, A. Clarke, I. Yashayaev, and P. Rhines, 2002: Convection and restratification in the Labrador Sea, 1990–2000. *Deep-Sea Res. I,* **49,** 1819–1835.

Legg, S., and J. McWilliams, 2001: Convective modifications of a geostrophic eddy field. *J. Phys. Oceanogr.,* **31,** 874–891.

Lilly, J. M., P. B. Rhines, M. Visbeck, R. Davis, J. R. N. Lazier, F. Schott, and D. Farmer, 1999: Observing deep convection in the Labrador Sea during winter 1994–1995. *J. Phys. Oceanogr.,* **29,** 2065–2098.

——, ——, F. Schott, K. Lavender, J. Lazier, U. Send, and E. D'Asaro, 2003: Observations of the Labrador Sea eddy field. *Progress in Oceanography,* Vol. 59, Pergamon, 75–176.

Marshall, J., and F. Schott, 1999: Open-ocean convection: Observations, theory and models. *Rev. Geophys.,* **37,** 1–64.

Mauritzen, C., and S. Hakkinen, 1999: On the relationship between dense water formation and the "Meridional Overturning Cell" in the North Atlantic Ocean. *Deep-Sea Res. I,* **46,** 877–894.

Maxworthy, T., and S. Narimousa, 1994: Unsteady, turbulent convection into a homogeneous, rotating fluid, with oceanographic applications. *J. Phys. Oceanogr.,* **24,** 865–887.

——, D. J. Torres, and R. A. Clarke, 2002: Hydrography of the Labrador Sea during convection. *J. Phys. Oceanogr.,* **32,** 428–457.

Prater, M., 2002: Eddies in the Labrador Sea as observed by profiling RAFOS floats and remote sensing. *J. Phys. Oceanogr.,* **32,** 411–427.

Rhein, M., and Coauthors, 2002: Labrador Sea Water: Pathways, CFC inventory, and formation rates. *J. Phys. Oceanogr.,* **32,** 648–665.

Send, U., and J. Marshall, 1995: Integral effects of deep convection. *J. Phys. Oceanogr.,* **25,** 855–872.

Smethie, W. M., and R. A. Fine, 2001: Rates of North Atlantic Deep Water formation calculated from chlorofluorocarbon inventories. *Deep-Sea Res.,* **48,** 189–215.

Spall, M. A., 2003: On the thermohaline circulation in flat bottom marginal seas. *J. Mar. Res.,* **61,** 1–25.

——, 2004: Boundary currents and water mass transformation in marginal seas. *J. Phys. Oceanogr.,* **34,** 1197–1213.

——, and D. C. Chapman, 1998: On the efficiency of baroclinic eddy heat transport across narrow fronts. *J. Phys. Oceanogr.,* **28,** 2275–2287.

——, and R. S. Pickart, 2001: Where does dense water sink? A subpolar gyre example. *J. Phys. Oceanogr.,* **31,** 810–826.

Straneo, F., 2006: Heat and freshwater transport through the central Labrador Sea. *J. Phys. Oceanogr.,* **36,** 606–628.

——, M. Kawase, and R. S. Pickart, 2002: The effects of wind on convection in strongly and weakly baroclinic flows with an application to the Labrador Sea. *J. Phys. Oceanogr.,* **32,** 2603–2615.

——, R. S. Pickart, and K. Lavender, 2003: Spreading of Labrador Sea Water: An advective-diffusive study based on Lagrangian data. *Deep-Sea Res. I,* **50,** 701–719.

Talley, L. D., 2003: Shallow, intermediate, and deep overturning components of the global heat budget. *J. Phys. Oceanogr.,* **33,** 530–560.

——, and M. S. McCartney, 1982: Distribution and circulation of Labrador Sea water. *J. Phys. Oceanogr.,* **12,** 1189–1205.

Visbeck, M., J. Marshall, and H. Jones, 1996: Dynamics of isolated convective regions in the ocean. *J. Phys. Oceanogr.,* **26,** 1721–1734.